Modelling EM-Coupling on Electrical Cable-Bundles with a Frequency-Domain Field-to-Transmission Line Model Based on Total Electric Fields

J-P. Parmantier[1], C. Guiffaut[2], D. Roissé[3], C. Girard[3], F. Terrade[4], S. Bertuol[1], I. Junqua[1], and A. Reineix[3]

[1]ONERA/DEMR, Université de Toulouse, F-31055 Toulouse - France
[2]CNRS-XLIM Institute, University of Limoges, Limoges - France
[3]AxesSim, Strasbourg, France
[4]Dassault Aviation, Saint-Cloud, France

Corresponding author: J-P. Parmantier (e-mail: jean-philippe.parmantier@onera fr).

ABSTRACT This article deals with modelling of EM-coupling on cable-bundles installed in 3D structures. It introduces a modified-Field-to-Transmission-Line model for which the specificity is to account for the reciprocal interaction between EM-fields and induced currents by considering equivalent total field sources. The first part of the paper is devoted to the derivation of this model starting from Agrawal's classical Field-to-Transmission-Line applied on a two-wire Transmission-Line and leads to a Transmission-Line model in which the signal-wire is now referenced to a fictitious surrounding cylinder acting as a return conductor. The modified-Field-to-Transmission-Line model is then obtained by modifying this derived-model in such a way that it is made compatible with numerical approaches and tools based on Agrawal's Field-to-Transmission-Line model. This modification involves a k_L coefficient equal to the ratio of the two per-unit-length inductances of the classical and derived Field-to-Transmission-Line models. Validations of this modified formulation clearly show the capability of this model to predict precise wire responses including EM-radiation losses. The second part of the paper is devoted to its extension to Multiconductor-Transmission-Line-Networks. The process relies on the capability to define an equivalent wire model of the cable-bundle in order to derive the k_L coefficient and to numerically evaluate equivalent total field sources. Validation of this extrapolation is presented on a real aircraft test-case involving realistic cable-bundles in order to assess the potentiality of the method for future problems of industrial complexity.

INDEX TERMS Transmission-lines, Multiconductor-Transmission-line-Networks, MTLN, Thin-Wire Model, Field-to-Transmission-Line, FTL, Cable-bundles, Cable-Networks, Electromagnetic Compatibility, EMC.

I. INTRODUCTION

Field-to-Transmission-Line (FTL) [1] is a well-known frequency-domain approach to model Multiconductor Transmission Lines (MTL) [2] in 3D structures and any types of electrical cable-bundles submitted to an Electromagnetic (EM) field. This model can be easily extended to Multiconductor-Transmission-Line-Networks (MTLN) [3]. Its main advantage is to make it possible MTLN calculations separately from 3D calculations. When applied in a numerical modelling process, the incident EM fields at the level of the wires, scattered by the whole 3D structure, can thereby be calculated and collected in the 3D model on the routes of MTLs but in the absence of the MTLs (Multiconductor Transmission-Lines). Then, they can be introduced as source-terms for the MTL-models. Several formulations of FTL model exist but Agrawal's formulation [4] based on incident tangential electric fields is the most appropriate for 3-dimensional (3D) numerical applications. The main interest of Agrawal's model from an EM-numerical modelling perspective is that the source-terms are tangent to the cable-routes, which avoids the constraint of having to define transverse field components like in the two other well-known classical FTL models, Taylor [5] and Rachidi [6].

The field of MTLN applications is very large. As far as cable-bundles are concerned, the interest for FTL is that the incident-field source-terms can be approximated as identical for all the wires of the MTL model. Therefore, an average incident field can be collected on the main route of the wiring

called the "central path" running along the center of the bundle network cross-sections. Besides, the position of electric cables in real cable-bundles is barely controlled. It generally varies along the bundle-path, making this average incident-field a relevant approximation of the incident-field distribution at the place of wires in the cable-bundle cross-section. Nevertheless, such an approximation is not valid for other types of MTLs such as power-lines for which several central paths associated to the MTL wires have to be defined because of the distance between wires. EM-coupling on cable-bundles in 3D structures has been the subject of several applications of Agrawal's FLT model ([7], [8], [9], [10]) and is now widely applied in laboratories and industry (Fig. 1). It is appropriate for the design of cable-bundles and installation for Electromagnetic Compatibility (EMC)-resilience, making it possible to optimize parameters such as cable-types, cable-shields, segregation distances, etc… More specifically, in industry, such calculation capabilities are particularly useful in the perspective of the regulation on wiring installation [11].

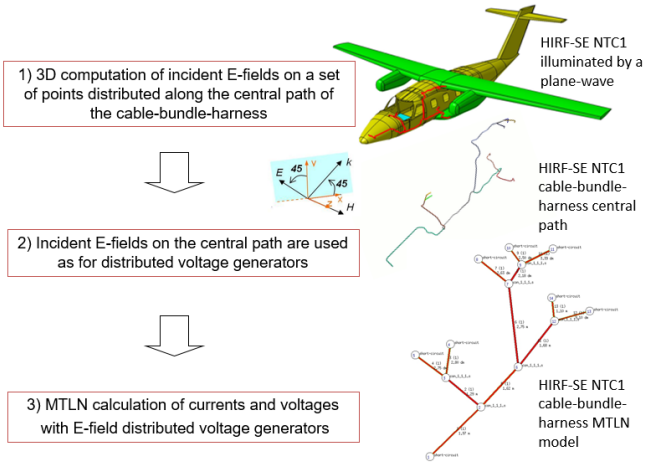

FIGURE 1. Example of FTL main calculation steps - Application on the HIRF-SE NTC1 test-case [9]– The aircraft is illuminated by a plane-wave. EM-fields scattered by the aircraft geometry are collected on the central path of the wiring and become incident fields for the MTLN problem

As far as 3D modelling is concerned, Finite Difference Time-domain (FDTD) remains one of the most robust techniques for calculating EM fields and electrical currents inside complex 3D structures. To this extend, FDTD has many advantages. First, in terms of meshing of complex internal geometry, the Cartesian grid can be generated by simple and efficient procedures on which refinement and correction are very limited compared to other methods based on conformal meshes. Second, the method easily copes with parallel computation techniques for addressing very large resource-demanding problems. Third, the method being widely spread in the EMC modelling community, it takes advantage of the availability of a large set of physical models, relevant for EMC analysis (dispersive volume and surface materials, thin wires, slots, absorbing conditions…). The EMC applications of this method range from any type of transport to ground systems. This is why, even for a frequency formulation approach of FTL, this 3D time domain technique remains fully relevant for providing the required MTLN source inputs ([7], [9]) (after Fourier transform). This is why, as far as 3D Maxwell computation is concerned, the focus of this paper will be on FDTD for providing reference results and inputs to FTL models.

Nevertheless, one of the main limitations of the FTL model is that it does not account for the reaction of the currents induced by Transmission-Lines (TLs) onto the incident EM-fields. EM-coupling models on cable-bundles thereby result of incident fields only but scattered fields resulting from the induced current cannot be calculated. Such an approximation is known to be sufficient as far as EM-radiation losses of the cable-bundle are negligible compared to other TL-losses.

One obvious way to account for this current reaction is to include cable models in 3D Maxwell-equations numerical models, considering for example time-domain numerical schemes for which the exchange of currents and EM-fields can be performed in both directions at each time step. To this extent, Holland's thin-wire model [12] or its derived-oblique models ([13], [14], [15]) are a widespread operational implementation of this concept for which the formulations are analogous to TL-equations. However their extension to multiconductor networks is difficult and the attempts to directly deal with MTL models embedded in Maxwell's equation still suffer from significant limitations such as uniform medium or large distance between wires in the perspective of EM-coupling on realistic cable-bundle architectures [16]. Even if those limitations of time-domain hybridization techniques can be overcome with hybridization techniques coupling both Maxwell-equations and MTL-equation [17], there is still a major difference with the frequency-domain FTL model. Indeed, the time-domain formulation makes it impossible the main operational advantage offered by the frequency-domain formulation of FTL: the capability of separating the calculations of the EM-field source terms and the MTLN response with a 3D software and a MTLN modelling tool respectively.

In this paper, we are thereby interested in investigating a possible way to overcome the FTL limitations while preserving its incontestable advantages. Our approach is in three steps. The first step consists in revisiting the theoretical background of FTL on single-wire-TLs and puts it in perspective of the thin-wire model used in 3D modelling in order to solve this current-on-field reaction limitation of FTL. The second step deals with the research of a modified-FTL formulation in order to be able to use the usual FTL calculation process and associated numerical tools. The third objective is to extend this modified-FTL model derived on single-wire-TLs to MTLN models, which is essential for industrial complexity applications.

To this extent, the paper is structured as follows. Section II establishes the theoretical developments of the modified

FTL-model in the frequency-domain, based on a single-wire-TL model made of two wires illuminated by an incident EM-field. In Section III, numerical validations of the modified-MTL model are made on several fully controlled configurations of single-wire-TL networks, for both EM-field and lumped voltage generator excitations. Section IV presents a modeling process to extend the modified-FTL model to cable-bundle configurations. A demonstration application is presented on the wiring harness of a real aircraft. Finally, Section V concludes on the relevance of the modified-FTL model for future applications on complex and realistic cable-bundle configurations.

II. DERIVATION OF THE MODIFIED-FTL MODEL FOR A SINGLE-WIRE-TL CONFIGURATION

A. PROBLEM TO SOLVE

Our theoretical development starts from a reminder of the demonstration of the first TL-equation applied on the same single-wire-TL geometry as in [1]. This TL is made of two parallel wires: a "signal-wire" and a "return-wire", each of them having the same length ℓ and radiuses a_s and a_r respectively (Fig. 2). The distance between the centres of the two wires is d.

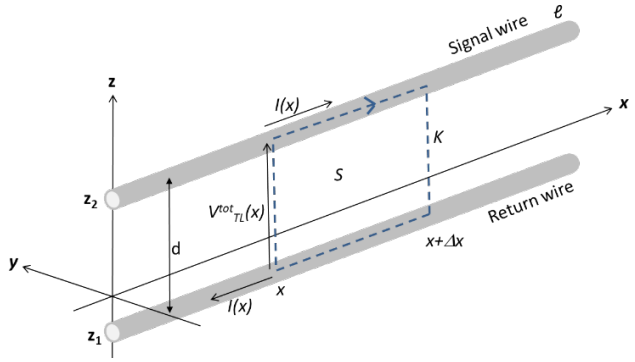

FIGURE 2. Geometry of the single-wire-TL problem. Identification of the surface *S* and its contour *K*.

In this paper, we do not make any restriction on a_s and a_r with respect to d since we do not explicitly need to calculate the per-unit-length (p.u.l.) inductance and capacitance parameters of the TL. The signal-wire has a p.u.l. resistance R_{signal} and the return-wire has a p.u.l. resistance R_{return}. x represents the longitudinal direction of the wires, y their transverse direction and z the direction normal to x and y in the plane of the two wires. The electrical current in the wires, $I(x)$, is in the x direction and the only restriction of this model is that $I(x)$ is supposed to be uniformly distributed into the cross-section of the two wires. This restriction is not a limitation in terms of precision of the results and demonstration of the method. It just means that our model does not account for redistribution of currents inside wires such as skin effect. If needed, such effects can be accounted for by adding specific frequency-dependent impedance models that particularly include loss models in the TL p.u.l. parameters. $V_{TL}^{tot}(x)$ is the voltage between the wires. We will see later on in this paper that the "*tot*" subscript stands for total EM-field related quantities. The objective of the derivation is to calculate $I(x)$ on the signal-wire.

B. APPLICATION OF THE FARADAY LAW

The theoretical developments presented in this paper all start from the Faraday Law applied on an open surface S as defined in Fig. 2 located in homogeneous free space medium geometry. In the frequency-domain, we can write:

$$\iint_S rot\vec{E}\cdot ds = \oint_K \vec{E}\cdot dl = -j\omega\mu_0 \iint_S \vec{H}\cdot dS \qquad (1)$$

where S is the open surface bounded by a contour K defined in our case as the rectangular contour along the x axis, between positions x and $x+\Delta x$, and the z axis, between positions z_1 and z_2 (Fig. 3).

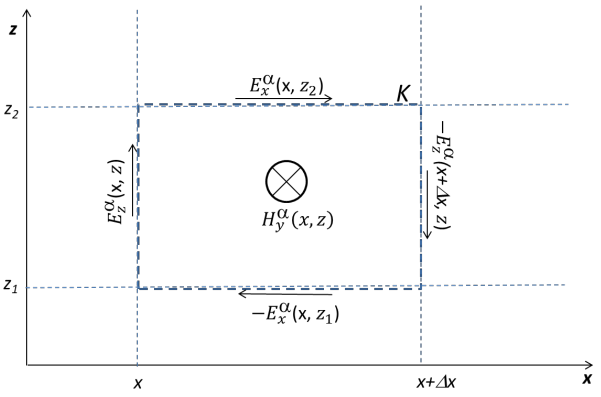

FIGURE 3. Surface S and contour of integration *K* used in the *x*-*z* plane for the application of the Faraday law.

In our approach, note that we define the return-wire as part of the "incident" problem and the signal-wire as part of the "scattered" problem. This means that the currents induced by the original incident EM-fields applied to the incident problem generate the total EM-fields that become the incident EM-fields at the level of the signal-wire as described in Fig.1.

We can therefore classically decompose the total EM-fields $\{E^{tot}, H^{tot}\}$ as the sum of the incident EM-fields $\{E^{inc}, H^{inc}\}$ (fields of the incident problem, i.e. in the absence of the signal-wire but in the presence of the return-wire) and the EM-scattered fields $\{E^{sca}, H^{sca}\}$ (fields due to the induced currents on the signal-wire). We thereby respectively write the electric and magnetic fields as:

$$\begin{aligned} E^{tot} &= E^{inc} + E^{sca} \\ H^{tot} &= H^{inc} + H^{sca} \end{aligned} \qquad (2)$$

Further in this paper, the EM field notations will be generalized as $E_\lambda^\alpha(x,y)$ and $H_\lambda^\alpha(x,y)$ (see Fig. 3) for the

electric and magnetic fields respectively, in which the subscript α will either stands for "*tot*", "*sca*" or "*inc*" and λ either for x, y or z directions. Then, the limit $\Delta x \to 0$ will be considered and the following simplification will be applied for any function f:

$$\lim_{\Delta x \to 0} \frac{\int_x^{x+\Delta x} f(x) \cdot dx}{\Delta x} = f(x) \tag{3}$$

With those definitions, the Faraday law in (1) applies either on the total, incident or scattered EM-fields (for convenience, the y coordinate will be removed from the notations) and leads to:

$$j\omega\mu_0 \int_{z_1}^{z_2} \left(H_y^{\alpha}(x,z)\right) \cdot dz = -\frac{dV_{z_1,z_2}^{\alpha}}{dx} - E_x^{\alpha}(x,z_2) + E_x^{\alpha}(x,z_1) \tag{4}$$

In which we define an equivalent voltage by:

$$V_{z_1,z_2}^{\alpha}(x) = -\int_{z_1}^{z_2} E_z^{\alpha}(x,z) \cdot dz \tag{5}$$

C. FORMULATION OF THE FTL EQUATIONS

Hereafter we remind quickly the main steps of the derivation of Agrawal's first FTL-equation since it will be the basis of our further derivations.

The application of (4) on the total EM-fields gives the first TL-equation based on Taylor's model as derived in [1]. According to the coordinate system of Fig. 3, we take $z_1 = 0$ and $z_2 = d$. The equivalent voltage to be considered is the total voltage and the source term is expressed in terms of the incident transverse magnetic field in S:

$$\left(R_{TL} + j\omega L_{TL}\right) I(x) + \frac{dV_{TL}^{tot}(x)}{dx} = -j\omega\mu_0 \int_0^d \left(H_y^{inc}(x,z)\right) \cdot dz \tag{6}$$

where

$$L_{TL} \cdot I(x) = \mu_0 \int_0^d \left(H_y^{sca}(x,z)\right) \cdot dz \tag{7}$$

and R_{TL} represents the p.u.l. resistance of the TL, classically equal to the sum of the p.u.l. resistances of R_{signal} and R_{return}. We have:

$$R_{TL} = R_{signal} + R_{return} \tag{8}$$

where

$$R_{signal} I(x) = E_x^{tot}(x,d) \tag{9}$$

$$R_{return} I(x) = -E_x^{tot}(x,0) \tag{10}$$

$$V_{TL}^{tot}(x) = -\int_0^d E_z^{tot}(x,z) \cdot dz \tag{11}$$

The application of (4) for the incident EM-fields gives:

$$j\omega\mu_0 \int_0^d \left(H_y^{inc}(x,z)\right) \cdot dz = -\frac{dV_{TL}^{inc}(x)}{dx} - E_x^{inc}(x,d) + E_x^{inc}(x,0) \tag{12}$$

with

$$V_{TL}^{inc}(x) = -\int_0^d E_z^{inc}(x,z) \cdot dz \tag{13}$$

The application of (4) to the scattered fields gives:

$$j\omega L_{TL} I(x) = -\frac{dV_{TL}^{sca}(x)}{dx} - E_x^{sca}(x,d) + E_x^{sca}(x,0) \tag{14}$$

with

$$V_{TL}^{sca}(x) = -\int_0^d E_z^{sca}(x,z) \cdot dz \tag{15}$$

defined as the "*scattered voltage*" [1].

In (6) we can also introduce the following property:

$$V_{TL}^{tot}(x) = V_{TL}^{inc}(x) + V_{TL}^{sca}(x) \tag{16}$$

Then combining (6) and (12) we find the well-known Agrawal-formulation for which we remind that the voltage to be considered is the scattered voltage and the source term is expressed in terms of tangential incident electric fields at the level of the signal and return-wires:

$$\left(R_{TL} + j\omega L_{TL}\right) I(x) + \frac{dV_{TL}^{sca}(x)}{dx} = E_x^{inc}(x,d) - E_x^{inc}(x,0) \tag{17}$$

The 2nd transmission line equation is obtained in a way entirely similar to the one presented in [1]. The introduction of the scattered voltage in the 2nd TL-equation formulated according to Taylor's model provides the 2nd Agrawal-equation that does not contain any right hand-side. We have then:

$$\left(G_{TL} + j\omega C_{TL}\right) V_{TL}^{sca}(x) + \frac{dI(x)}{dx} = 0 \tag{18}$$

where

- G_{TL} is the TL p.u.l. conductance,
- C_{TL} is the TL p.u.l. capacitance

The demonstration of (18) will not be reported in this paper since the EM-field-related source terms only appear in the 1st TL-equation.

From an application point of view, even if the Agrawal-formulation involves scattered voltages that do not have real existence, it is important to remember that the currents $I(x)$

remain the "real" electrical currents. Besides the total voltage as defined in (11) (real voltages at the ends of the TL) can always be obtained from *I(x)* by applying Ohm's law as far as end-load impedances are known.

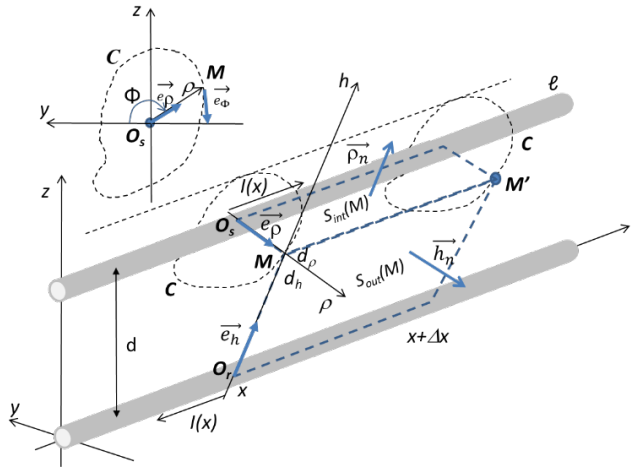

FIGURE 4. The single-wire-TL problem with a fictitious cylinder surrounding the signal-wire. Various coordinate systems referred to the return-wire and the fictitious cylinder.

D. FORMULATION OF A MODEL INDEPENDENT OF THE RETURN-CONDUCTOR

We consider the same geometry as the one in Fig. 2 with the signal-wire parallel to the return-wire and a separation distance *d* between the wires. We consider now a small fictitious cylinder with an arbitrary cross-section surface of contour *C*, extending in the *x* direction around the signal-wire path (Fig. 4). In the same way we would generate a unified TL-model of a shielded cable with respect to a common reference conductor [18]; we thereby define three different TLs named as follows (even if the cylinder is a fictitious conductor, we will see later on that we can define a TL-like equations for the three related-domains):

- "Inner-TL", the TL made of the signal-wire with respect to the fictitious cylinder.
- "Outer-TL", the TL made by the fictitious cylinder with respect to the return-wire.
- "Reference-TL", the TL made by the signal-wire with respect to the return-wire (the TL defined in the previous paragraph for the FTL model).

As for (17), we start the derivation from the application of Faraday's law in its infinitesimal formulation (4). For this, we define three reference geometrical points: a point of origin O_s on the signal-wire and a point O_r on the return-wire, both of them at the position *x*, and a point *M* taken on the contour *C* of the cylinder at the same *x* position; the $\overrightarrow{O_sM}$ and $\overrightarrow{O_rM}$ vectors are perpendicular to the *x* direction.

We then define a cylindrical coordinate system local to the signal-wire with an origin in O_s. In this system, the ρ coordinate represents the position of *M* on the contour *C* and varies between 0 and d_ρ.

The line between point *M*, taken at position *x*, and point *M'*, taken at position $x+\Delta x$, allows us to decompose the surface of integration in two plane surfaces: one inner-surface, $S_{int}(M)$, and one outer-surface, $S_{out}(M)$. $S_{int}(M)$ is defined by the *x* direction and the $\vec{e}_\rho$ unit vector passing by O_s and *M*. $S_{out}(M)$ is defined by the *x* direction and the $\vec{e}_\rho$ unit vector passing by O_r and *M*. The *h* coordinate with respect to $\vec{e}_h$ varies between 0 and d_h. $\vec{\rho}_n$ and $\vec{h}_n$ vectors define the unit vectors normal to $S_{int}(M)$ and $S_{out}(M)$ respectively (the reader will pay attention not to make confusion with $\vec{e}_\rho$ and $\vec{e}_h$ definitions).

The application of (4) is made on the total EM-fields marching on the integration contours of the two $S_{int}(M)$ and $S_{out}(M)$ surfaces. In the same way as the derivation of (17), we find:

$$\begin{aligned}&E_x^{tot}(x,z=d)-E_x^{tot}(x,z=0)+\\&\lim_{\Delta x\to 0}\left(\frac{-\int_0^{d_h}\left(E_h^{sca}(x+\Delta x,h)-E_h^{sca}(x,h)\right)\cdot dh}{\Delta x}+\right.\\&\left.\frac{+\int_0^{d_\rho}\left(E_\rho^{sca}(x+\Delta x,\rho)-E_\rho^{sca}(x,\rho)\right)\cdot d\rho}{\Delta x}\right)+\\&j\omega\mu_0\left(\int_0^{d_h}\left(\vec{H}^{sca}(x,h)\cdot\vec{h}_n\right)\cdot dh+\right.\\&\left.\int_0^{d_\rho}\left(\vec{H}^{sca}(x,\rho)\cdot\vec{p}_n\right)\cdot d\rho\right)=E_x^{inc}(x,z=d)-E_x^{inc}(x,z=0)\end{aligned}\tag{19}$$

where two specific voltages terms can be defined:

$$\frac{dV_{out}^{sca}(x)}{dx}=\lim_{\Delta x\to 0}\frac{-\int_0^{d_h}\left(E_h^{sca}(x+\Delta x,h)-E_h^{sca}(x,h)\right)\cdot dh}{\Delta x}\tag{20}$$

the p.u.l. variation of the scattered voltage in the Outer-TL and

$$\frac{dV_{int}^{sca}(x)}{dx}=\lim_{\Delta x\to 0}\frac{-\int_0^{d_\rho}\left(E_z^{sca}(x+\Delta x,\rho)-E_z^{sca}(x,\rho)\right)\cdot d\rho}{\Delta x}\tag{21}$$

the p.u.l. variation of the scattered voltage in the Inner-TL. From (4), we have also:

$$\begin{aligned}&j\omega\mu_0\int_0^{d_h}\left(\vec{H}^{sca}(x,h)\cdot\vec{h}_n\right)\cdot dh=\\&-\frac{dV_{out}^{sca}(x)}{dx}-E_x^{sca}(x,h=d_h)+E_x^{sca}(x,0)\end{aligned}\tag{22}$$

By introducing (22) in (19), we finally obtain:

$$R_{signal} I(x) + j\omega\mu_0 \int_0^{d_\rho} \left(\vec{H}^{sca}(x,\rho)\cdot\vec{\rho}_n\right)\cdot d\rho + \frac{dV_{int}^{sca}(x)}{dx} = E_x^{inc}(x, z=d) + E_x^{sca}(x, h=d_h) \quad (23)$$

Now, the last step of the derivation is to calculate the averages of all the quantities of (23) by integrating them over the whole contour ***C*** of perimeter *P* and normalize them over *P*. For this, we introduce a curvilinear coordinate *u* allowing us to position point *M* anywhere over the ***C*** contour. We note that:

$$\oint_C du = P \quad (24)$$

For example, particular application of this fictitious surrounding cylinder is when the cylinder cross-section is circular and of radius R_c. In this case, the *u* variable becomes $du = R_c.d\Phi$ and $P = 2\pi R_c$.

We obtain:

$$\frac{\oint_C \frac{dV_{int}^{sca}(x)}{dx}\cdot du}{P} + R_{signal} I(x) + j\omega\mu_0 \frac{\oint_C \left(\int_0^{d_\rho} \left(\vec{H}^{sca}(x,\rho)\cdot\vec{\rho}_n\right)\cdot d\rho\right)\cdot du}{P} = E_x^{inc}(x, z=d) + \frac{\oint_C E_x^{sca}(x, h=d_h)\cdot du}{P} \quad (25)$$

In which we can introduce the following definitions:

- The average scattered voltage in the Inner-TL defined by:

$$\left\langle V_{int}^{sca}(x)\right\rangle = \frac{\oint_C V_{int}^{sca}(x)\cdot du}{P} \quad (26)$$

- The p.u.l. inductance of the Inner-TL defined by:

$$L_{TL,int} I(x) = \mu_0 \frac{\oint_C \left(\int_0^{d_\rho} \left(\vec{H}^{sca}(x,\rho)\cdot\vec{\rho}_n\right)\cdot d\rho\right)\cdot du}{P} \quad (27)$$

- The average scattered field on the *C* contour:

$$\left\langle E_x^{sca}(x)\right\rangle = \frac{\oint_C E_x^{sca}(x, h=d_h)\cdot du}{P} \quad (28)$$

In (25) we can also define an "*equivalent total tangential electric field*" at the level of the signal-wire as the sum of the incident EM-field at the wire-level and the average of the scattered tangent electric fields on the contour *C*:

$$\left\langle E_x^{tot}(x)\right\rangle = E_x^{inc}(x, z=d) + \left\langle E_x^{sca}(x)\right\rangle \quad (29)$$

Note that (28) is not null and that the integrals over C must not be confused with "vector circulation" over a contour. An interesting aspect is that this source term can be directly obtained with a 3D-calculation that includes the thin-wire model of the signal-wire and the return-wire (or reference return-conductor).

With those definitions, we can now write (25) in the following compact form:

$$\left(R_{signal} + j\omega\cdot L_{TL,int}\right)\cdot I(x) + \frac{d\left\langle V_{int}^{sca}(x)\right\rangle}{dx} = \left\langle E_x^{tot}(x)\right\rangle \quad (30)$$

As in (18), the second TL equation writes:

$$j\omega\cdot C_{TL,int}\cdot\left\langle V_{int}^{sca}(x)\right\rangle(x) + \frac{dI(x)}{dx} = 0 \quad (31)$$

where $C_{TL,int}$ is the p.u.l. capacitance of the Inner-TL.

These two equations can be introduced into any types of full wave solvers together with their specific meshed geometrical models. More specifically, (30) is obtained in this paper with a contour averaging but it can be also derived averaging over an area as well. The averaging process with the contribution of many electric field components increases accuracy, as observed for oblique thin-wire models in Cartesian meshes for which the 2D-symmetry for straight thin wires does not exist anymore and leads to non-uniform distributions of scattered electric field components around *C* [13].

In the continuation of this article, we will focus on the FDTD method and the analogy of (30) with Holland's thin-wire model [12] or its extensions for oblique-wire models implemented in the FDTD method ([13], [14]). The thin-wires are inserted in a Cartesian mesh and the tangential fields along the wires result from an averaging of the electrical fields in the surrounding FDTD cells very similarly to (30). Note that each field component calculated by the FDTD method can also be seen as an average field flux through a quad area. The average process applies even when the wires are located along a FDTD grid edge.

We want to stress the fact that the total field quantity in (29), implicitly applied at the wire-level must only be understood as an average of electric fields calculated around the wire; in other words, for lossless wires, this field is not equal to zero as the physics would impose it. Inside both thin-wire and Inner-TL models the update of the scattered field due to signal-wire induced-current is not made but both models allow this update outside the surrounding cylinder surface.

Besides, (30) and (31) have been obtained with the single-wire-TL configuration described in Fig. 2. However, as done in [1] for the derivations of Taylor's and Agrawal's FTL models, this model can be extended to any geometrical configuration of return-conductor. Thereby, in the following of this article, the return-wire will be replaced by any

structural geometry, for example a ground plane or a 3D surface of any geometrical shape.

In (30), note that the equation does not depend explicitly on the surrounding 3D-structure anymore unlike in (17). Indeed, in (17), we note that the presence of the return-conductor appears in the resistance and inductance p.u.l. parameters. Consequently, the Inner-TL model is of particular interest for real 3D geometrical configurations since it is independent from any reference taken on the 3D structure. Indeed, in realistic applications, the Reference-TL return-conductor of FTL is not easy to identify and generally needs to be approximated by a simplified geometry (the most usual one being a ground plane).

As far as the frequency scope validation is concerned, all TL-models are subject to the TEM mode approximation. For a single-wire TL made of a wire over a ground plane, a usual criterion is to have $\lambda_{min} > 10h$, where h is the height over the plane. Such a criterion applies for (17). For coaxial structures, this criterion extends to $\lambda_{min} > 10R$, where R is the radius of the cable-shield, allowing us to perform FTL-modelling beyond the usual criterion. Such a criterion applies for (30). Consequently, the Inner-TL model is less surrounding-geometry-dependent and applicable at higher frequencies than the Reference-TL model.

E. MODIFIED-FTL FORMULATION

Despite different source terms definitions in the right hand side in (17) and (30), we need to keep in mind that both equations are derived from the application of Faraday's law of the same problem and we observe that equations (17) (for the Reference-TL) and (30) (for the Inner-TL) have very similar equation forms. However, in order to make those two equations fully comparable, we have to reference (30) to the same return-conductor as in (17). This transformation is particularly required in order to account for the fact that the end loads are always connected between the signal-wire and the return-conductor. Such a transformation can be obtained mathematically if we make appear L_{TL} and C_{TL} instead of $L_{TL,int}$ and $C_{TL,int}$ in (30) and (31) respectively. For this purpose, we introduce the k_L coefficient defined as the ratio between the p.u.l. inductances of the Reference-TL and the Inner-TL respectively:

$$k_L = \frac{L_{TL}}{L_{TL,\text{int}}} \tag{32}$$

From (32) we derive the transformation of the p.u.l. capacitance assuming homogeneous medium:

$$C_{TL} = \frac{1}{v^2.L_{TL}} = \frac{1}{v^2.k_L L_{TL,\text{int}}} = \frac{C_{TL,\text{int}}}{k_L} \tag{33}$$

Then we multiply (30) by the k_L coefficient and we introduce (33) in (31). We then obtain the two equations of a specific FTL model that we will call "modified-FTL" in order to make the distinction with the classical FTL model:

$$\left(k_L R_{signal} + j\omega \cdot L_{TL}\right) \cdot I(x) + \frac{dV_{TL}^{eq}(x)}{dx} = k_L \left\langle E_x^{tot}(x) \right\rangle \tag{34}$$

$$j\omega \cdot C_{TL} \cdot V_{TL}^{eq}(x) + \frac{dI(x)}{dx} = 0 \tag{35}$$

In both (34) and (35) we introduce a new equivalent TL voltage definition:

$$V_{TL}^{eq}(x) = k_L \left\langle V_x^{tot}(x) \right\rangle (x) \tag{36}$$

Note that the modified-model involves an equivalent voltage definition, $V_{TL}^{eq}(x)$, which is not the real voltage (11). However both models provide the real current solution, *I(x)*. Besides, compared to (17) which uses incident electric fields (namely $E_x^{inc}(x,d) - E_x^{inc}(x,0)$) as right-hand-side term, (34) uses an analogous $k_L \left\langle E_x^{tot}(x) \right\rangle$ right hand side term.

In a way analogous to what is done in Agrawal's model in (17) and (18), the system of equations (34) and (35) matches a regular FTL model implementation. Especially, such a mathematical formulation enables us to use all the numerical tools and procedures already available for regular Agrawal FTL applications.

Two situations illustrate the equivalence with Agrawal's model which is an accurate and proven one as long as radiating effect can be neglected. Consider first the very low frequencies where inductive effects are neglected. Then subsists Ohm's law relationship in (17) and (34) only. In both cases, (17) and (34) become strictly equivalent:

$$R_{signal} I(x) = \left\langle E_x^{tot}(x) \right\rangle = E_x^{inc}(x,d) - E_x^{inc}(x,0) \tag{37}$$

At low frequency, TL-generated scattered electric fields are insignificant and the electric field of the reference conductor is taken into account into the $\langle \boldsymbol{E_x^{tot}} \rangle$ component calculated from 3D-modeling. Hence the k_L factor does not impact the resistive effect of the line.

Let us now consider a second situation of a conductor without losses and at low frequency band for which only inductive effects, but still without radiating fields due to TL, can be considered. Thenceforth, as systems (17) - (18) and (34) - (35) are valid to predict the true response, both left hand-sides become strictly equivalent and we have the following equality

$$k_L \left\langle E_x^{tot}(x) \right\rangle = E_x^{inc}(x,d) - E_x^{inc}(x,0) \tag{38}$$

From this point of view, the k_L factor defines the change of TL reference conductor making the equivalence from a neighbor total electric field $\langle \boldsymbol{E_x^{tot}} \rangle$ to incident electric fields on the TL signal and return conductors.

F. CONSEQUENCE ON THE TL-END-IMPEDANCES

We observe that (34) shows that the R_{signal} series impedance is multiplied by the k_L coefficient. At low frequency, for a TL short-circuited at both-ends, the TL-network model may be defined by localising the total resistance of the TL, $R_{signal} \cdot \ell$, at one end of the TL, the TL-model now becoming lossless. If a finite impedance $Z_{TL,1}$ terminates the TL, it will be then added in series with this localized TL-total-resistance. Consequently, if two $Z_{TL,1}$ and $Z_{TL,2}$ end-impedances terminate the TL-network model, they will have themselves to be multiplied by the k_L coefficient.

III. NUMERICAL VALIDATION OF THE MODIFIED-FTL MODEL ON CANONICAL TEST-CASES

A. CANONICAL TEST-CASES AND NUMERICAL METHODS USED

We will now validate the FTL model on canonical configurations of lossless single-wire-TL-networks over PEC ground planes. These configurations will show several advantages with respect to our validation objective. First, this single-wire-TL simplification allows us comparison with 3D-full-wave simulations and thin-wire models. As far as our validations are concerned, another main advantage of these configurations on ground planes is also that the Reference-TL-model p.u.l. parameters are calculated with precision because the return-conductor (the ground-plane) is perfectly identified. The last interest is that the wire networks will be challenging for our validations. Indeed, the single-wires will behave as receiving or emitting antennas. We will therefore be able to investigate to which extent our modified-FTL model has the capability to model EM-radiation losses, being known that this is not achievable by classical FTL.
In order to capture the wideband physics of the responses, all results will be analysed in the frequency-domain on a large frequency range. In what follows, all canonical problems will be numerically simulated with three methods:

- Full-wave method: i.e. a 3D FDTD calculation in the time-domain in which the wires under test are present in the 3D model as thin-wire models and parts of the 3D numerical resolution. This calculation is considered to provide the reference wire-current results after having been Fourier-post-processed in the frequency-domain.
- FTL method: i.e. the classical Agrawal FTL method for which the source terms are provided by 3D FDTD calculations that do not include the wires under test and provide incident electric fields along the wire-routes after having been Fourier-post-processed in the frequency-domain (17). Then those incident electric fields are used as voltage generators in a MTLN model for a regular FTL calculation process.
- Modified-FTL method: i.e. the modified-FTL method for which the source terms are calculated with 3D FDTD calculations in the time-domain that include the wires under test and provide total equivalent electric fields along the wire routes (36) after having been Fourier-post-processed in the frequency-domain. Then those total electric fields are used as voltage generators in a MTLN calculation.

The FDTD tool for all 3D simulations is the TEMSI-FD software [19]. The calculation of the TL-network response has been made with the CRIPTE software that allows FTL calculation procedure [20].

B. SINGLE-WIRE VALIDATION TEST-CASE

Presentation of the test-case

The first geometrical configuration is pictured in Fig. 5. It is made of a single wire of radius 0.1 mm and length 2 m, called "victim-wire", running in parallel in the x direction on the upper-side of a PEC ground plane of finite-dimensions (1.5 m x 1.5 m) at a height h=10 cm. Two vertical wires of similar radiuses connect it to the ground plane. At this level, two lumped resistances equal to 1 Ω have been considered. This value allows approaching a low impedance condition of the TL (close to short-circuit) while providing losses large enough to correctly damp all time responses to zero and to obtain finite amplitude peaks in the frequency-domain.

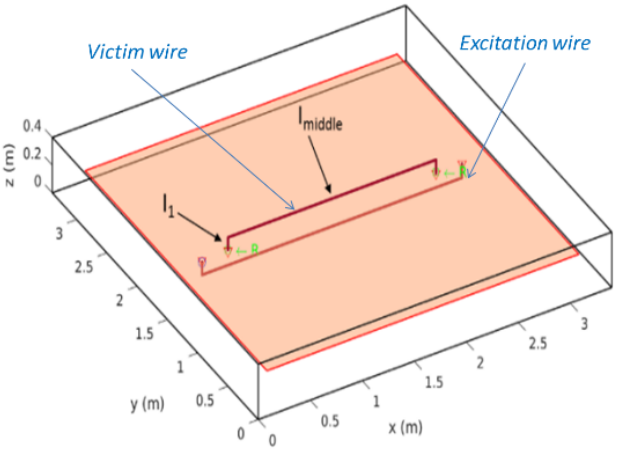

FIGURE 5. Geometrical configuration used for the validations on a single-wire-TL test-case. The rectangular box indicates the position of the PML layers used in the FDTD model.

On the underneath side of the PEC plane, in the same x-z plane as the victim-wire, another wire, called "excitation-wire", with the same radius and height as the victim-wire, is running in the x direction. This wire is connected to two vertical wires as above the ground plane but, this time, with a resistive load of 50 Ω on the left hand side (small x-values end) and a short-circuit on the right hand side (large x-values end). In this geometry, a lumped voltage generator is applied at the level of the ground-plane either on the left-hand-side extremities of the victim-wire or on the excitation-wire. Note that the two types of excitations, even localized, generate scattered EM-fields in the whole 3D domain.

In those tests, we observe the current on the victim-wire at two positions: at the left hand side extremity ("I_1") and in the middle length of the wire ("I_{middle}"). To be consistent with the incident problem definition, the excitation-wire is always included in the 3D model.
In both FTL and modified-FTL methods, note that the field source terms must be applied on the horizontal part as well as on the two vertical parts connecting the wire on the PEC ground planes. In the horizontal wire part, the p.u.l. parameters are approximated as the p.u.l. parameters of a wire over an infinite ground-plane. The vertical wires are approximated by TLs having the same p.u.l. electrical parameters as these of the horizontal line (usual conic antenna approximation [21]). The cell-size in all FDTD models is chosen equal to 2 cm. Perfectly-Matched-Layers (PML) absorbing conditions surround the calculation-domain box of size 3.4 m x 3.4 m x 0.4 m. Time-domain calculations have been made by applying successively on one of the two wires a lumped voltage generator. Each of them has the same Gaussian waveform whose frequency spectrum extends up to 300MHz. This frequency is consistent with the validity of the TL model, using the arbitrary criterion, $\lambda_{min} > 10h$. Then all currents induced on the victim-wire calculated with the three methods have been Fourier-transformed in order to compare them in the frequency-domain. The frequency sampling has been made such that of each frequency resonance peak is sampled with about a 400- kHz step, which provides sufficient precision of the resonance peak amplitudes (about 50 frequencies per peak). Finally, all currents obtained by the three methods have been normalized to the Gaussian waveform.

Field excitation by the "excitation" wire

This configuration is called "field excitation" since the incident field applied on the victim-wire is generated by the current developed on this excitation-wire, underneath the ground plane. More precisely, the current forced on the excitation-wire, combined with the currents induced on the finite-dimensions ground-plane surface, scatters EM-fields that become incident fields at the level of the victim-wire route as in Fig. 1's calculation process. The lumped generator, including the 50 Ω resistive load, is applied on the left-hand-side extremity of the excitation-wire at the level of the ground plane. The current responses, I_1 and I_{middle}, obtained by the three methods at the two observation test-points on the victim-wire are presented in Fig. 6, in logarithmic scale on the full frequency variation range and in linear scale in the frequency resonance range in order to be able to observe in details the resonance peaks.

On the one hand, we observe that the FTL method gives as expected very satisfactory results in the whole frequency range (see upper plot in logarithmic *x*-scale). Especially, it perfectly works from DC up to about 20 MHz, i.e. for quasi-static regime. However, in the resonance regime of the wire, even if the resonance frequencies are well predicted, we observe that the peaks have significant amplitude differences with the reference results (see lower plots in linear *x*-scale in which FTL provides larger amplitude peaks than the reference full-wave method). On the other hand, the modified-FTL method entirely predicts the reference results on the whole frequency band, including the resonance range. The comparison is almost perfect at the left hand side extremity (I_1) since the modified approach results perfectly overlap the reference calculated current (Fig. 6(a)).
Even if the comparison if very acceptable, we do not observe such a perfect matching in the middle of the wire (I_{middle}) but we note that this discrepancy also appears in Agrawal's classical FTL (Fig. 6(b)). So far, we explain this discrepancy by the fact that the FTL and MTL models remain model approximations of real wiring EM scattering problems. In [1], the authors clearly explain that even if the TL-current modes are the main current modes at the terminations of the TL, the total current also includes the antenna-mode currents anywhere on the line. In the general case of wires over a ground plane, the antenna-mode currents are much smaller than TL-mode currents because of the symmetry brought by the ground plane. Nevertheless, the weight of the antenna mode current becomes larger as the height of the wire increases with respect to the ground plane (in terms of number of wavelengths). Such a phenomenon is clearly observed in Fig. 6(b)'s plots for which both FTL models (with incident and total E field) cannot fully reproduce the frequency variation of the full FDTD response, unlike at the extremities of the TL as observed in Fig. 6(a). Besides, note that the agreement with the reference full-wave FDTD method is better with the modified-FTL model than with the FTL model because the absence of antenna mode is limited inside the surrounding cylinder and because the scattered-field update capability outside this cylinder is able to catch the physics of this antenna mode. In addition, we also explain the modified-FTL response discrepancy by the fact that the multiplication of the TL end-impedances by the k_L factor is only relevant at cable ends when the impedance values are explicitly known. However, in network configurations, impedances to be considered at connections or outside the real TL-ends should theoretically account for the equivalence impedances brought by the rest of the network.

Direct excitation of the "victim" wire voltage

A lumped generator including a 1 Ω resistive load is now applied directly on the left-hand-side extremity of the victim-wire (wire over the ground plane) at the level of the ground plane. From a validation point of view, this configuration is more challenging since no incident field is really applied on the victim-wire route as in the previous excitation configuration. Besides, in this case, the response of the victim-wire can be directly obtained from a straightforward frequency-domain TL-model by exciting the victim-wire with a 1V voltage generator. Nevertheless, we can also apply the modified-FTL model and see the effect of the equivalent total field source terms (here equal to the average scattered tangential electric field part around the wire only). Note

however that, for completion of the source-term model, the lumped voltage generator must be added as a localized incident field applied at the victim-wire left hand-side.

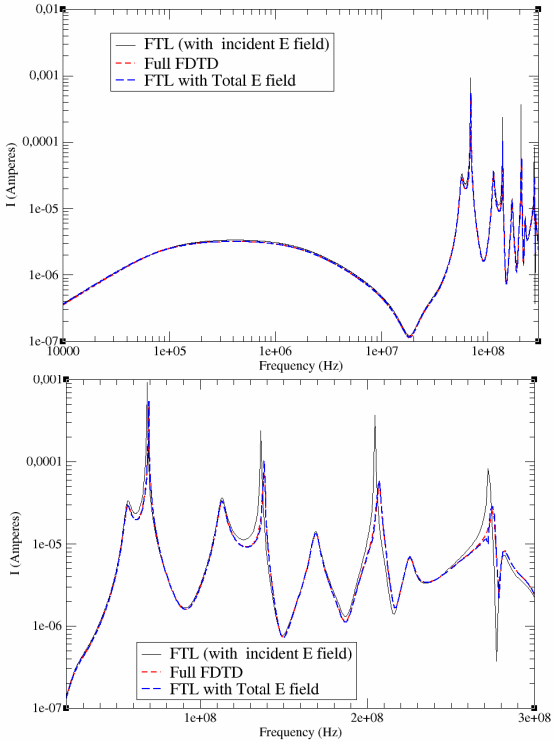

(a) Currents obtained at the left-hand-side extremity I_1, log scale (top) and linear scale (down).

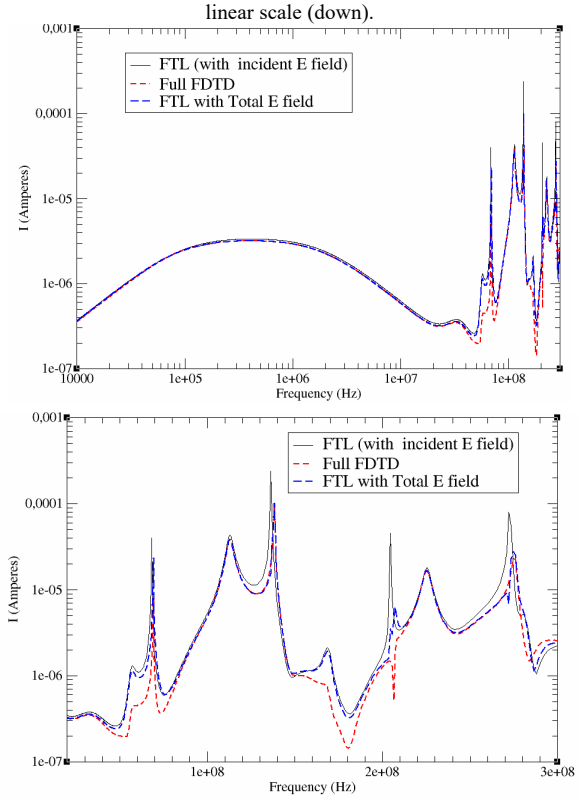

(b) Currents obtained in the middle of the wire I_{middle}, log scale (top) and linear scale (down).

FIGURE 6. Field excitation configuration (local voltage generator on the excitation-wire) – Comparisons of currents obtained between full-3D (label "*Full FDTD*"), classical Agrawal's method (label "*FTL (with incident E field)*") and modified-FTL method (label "*FTL with Total E field*").

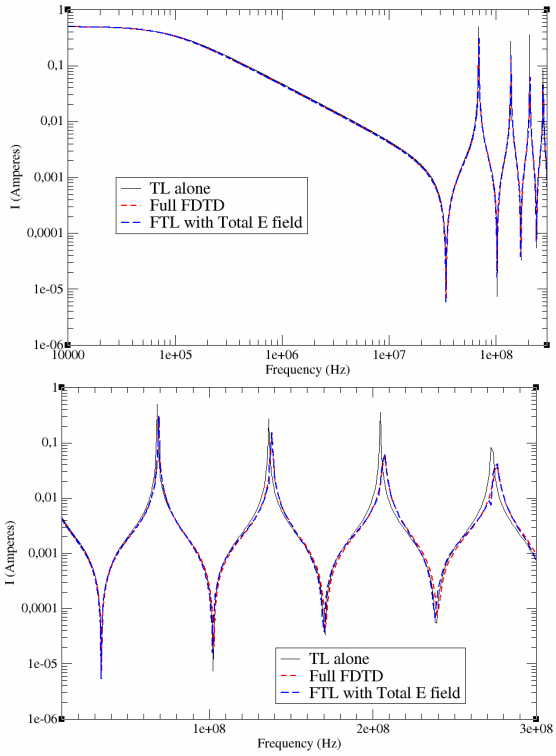

(a) Currents obtained at the left-hand-side extremity I_1, log scale (top) and linear scale (down).

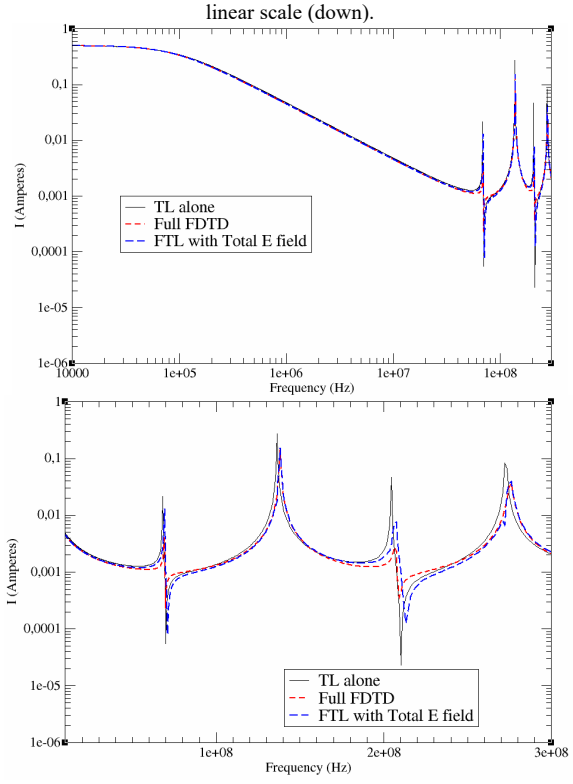

(b) Currents obtained in the middle of the wire I_{middle}, log scale (top) and linear scale (down)

FIGURE 7. Victim-wire voltage excitation configuration (local voltage generator on the victim-wire) - Comparisons of currents obtained between full-3D (label "*Full FDTD*"), classical TL model (label "*TL alone*") and modified-FTL method (label "*FTL with Total E field*").

In terms of result comparisons, the conclusions are the same as for the former field illumination configuration. Especially, in this configuration, the modified-FTL method clearly highlights the EM-radiation losses on the wire. We even observe that the current at the middle (Fig. 7(b)) is better predicted than in the excitation configuration, certainly because a pure differential mode is excited on the TL and no antenna mode currents have to be considered (which does not mean that this configuration does not scatter EM fields !).

B. BRANCHED NETWORK CONFIGURATION

The previous test-case concerned only one single-TL. Here, we want to evaluate the robustness of the modified-FTL model for branched network configurations (even if the reader must note that the previous single-wire-TL test-case already included network aspects because of the connection of the two small vertical parts to the horizontal part of the wire). In this new geometrical configuration, the PEC ground plane dimensions are 2.3 m x 1.7 m. Other main dimensions are reported in Fig. 8. A straight wire of radius 5 mm is connecting two metal boxes at the level of two connection points called "*connector A*" and "*connector B*". A transverse wire of radius 5 mm connects this straight wire at one extremity and the ground plane to a connector C with a vertical wire at the other extremity.

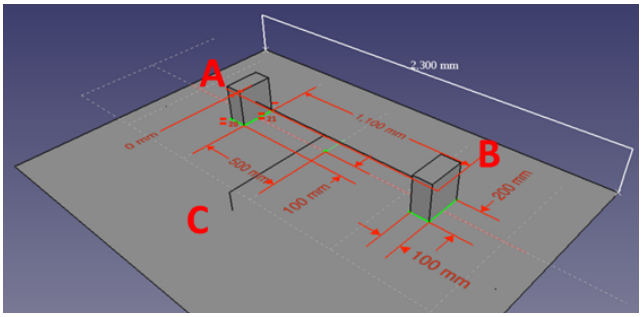

FIGURE 8. Geometrical configuration used for the validation on branched networks.

As for the previous single-wire-TL test-case, an excitation-wire is running under the ground-plane in the direction of the upper-ground straight wire. All wires, including the excitation-wire, are at a 10-cm height above or below the PEC ground plane. The mesh size in the 3D-model is 2.5 cm. Note that the two metal boxes are meshed in the 3D model as well as the excitation-wire in the incident field problem. The box models significantly contribute to the large amplitude of the incident tangential electric fields at their level. The same Gaussian waveform lumped voltage generator as in the previous single-wire test-case is applied. With the 10-cm height of the victim-wire, the TL model is strictly valid up to 300 MHz. However, we have extended the analysis up to 600 MHz in order to show if the modified-model could predict the frequency damping due to EM radiation losses observed in the reference full-wave results. Note indeed that the modified-FTL model has a larger frequency validity because the inner-TL is referenced to the close surrounding cylinder sized by the Cartesian mesh. Considering the 2.5-cm mesh size, we estimate its validity approximately up to 600 MHz.

Fig. 9 presents the currents obtained at connector A in two load configurations when all wire-ends are either on 50 Ω or on short-circuits. In the 50 Ω configuration, full-3D FDTD reference and FTL-model results correctly match those obtained with the modified-FTL model. In this configuration, the 50 Ω loads mask the EM radiation losses (even if the reader will note that the amplitude of the peaks with the FTL method is slightly larger).

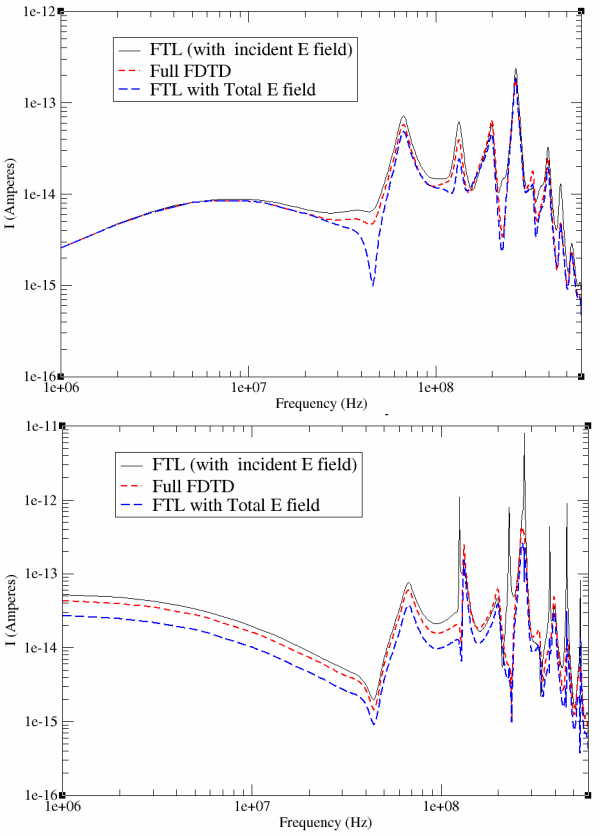

FIGURE 9. Currents at end A on the branched network configuration. All extremities loaded on 50 Ω (top) and short-circuit (down). Currents obtained between full-3D ("*Full FDTD*"), classical Agrawal's method ("*FTL (with incident E field)*") and modified-FTL method ("*FTL with Total E field*").

The reader may note that the modified-FTL response displays a very sharp attenuation peak at 45 MHz that is also identifiable in both the classical FTL and the full-FDTD responses, but with a much lower attenuation amplitude. This sharp dip results of a quasi-perfect compensation of two opposite waves occurring with this very specific geometry configuration. The most likely origin of such a very sensitive phenomenon is that the modelling implementation is based on procedures combining different numerical resolution schemes in time and frequency domains together with their

inherent numerical approximations. More specifically, the fact that EM field unknowns are discrete in the full-wave method whereas current and voltages are continuous in the TL method or the fact that the FDTD schemes are known to be dispersive are the currently suspected reasons. Nevertheless, the relevance of such comparisons must rely on the fact that all the resonance peaks are well calculated, which is the case in Fig. 9. This sharp dip phenomenon will have all the less impact for wide band analysis of real complex problems (see aircraft example in section IV). In short-circuit configuration instead, the same conclusions as for the previous single-wire TL test-case can be drawn. The modified-FTL model allows us to reproduce EM-radiation losses in the resonance region of the wire responses. The small shift in amplitude observed at low frequencies with the two FTL models is explained by Fourier-transform issues due to time-domain signals not fully returned to zero.

IV. GENERALIZATION OF THE MODIFIED-FTL MODEL TO MTLN

A. OBJECTIVE AND MTL-EXTENSION PROCESS

In addition to the capability to provide the response at cable-wire levels in bundle, the other big advantage of Agrawal's FTL model is to provide distributed source terms independently from the type of wiring since they are derived from electric incident fields, i.e. electric fields in the absence of the wiring. With this capability, very efficient and now fully operative hybridized numerical modelling processes have been developed in the frequency-domain in order to address problems of industrial complexity. Our objective is now to reach such a capability with our modified-FTL model.

So far, we have derived and numerically validated the modified-FTL model for single-wire-TLs only. We must also stress the fact that the derivation of the equivalent source term in (34) depends on the wiring configuration since (36) requires adding the field terms scattered by the signal-wire on the surface of the fictitious cylinder to the incident fields. Up to this point of this article, the interest of this modified-FTL model is limited to a theoretical peculiarity. From an application point of view, the modified-FTL has even no real interest for single-wire-TL configurations as far as such configurations can be directly modelled as thin-wire models in 3D numerical schemes! The interest of the modified-FTL may thereby exist only and only if it can be applied to cable-bundle configurations in order to overcome modelling domains for which FTL has limitations.

Nevertheless the single-wire-TL derivation sets the background of a modelling process in which strong interaction with EM-scattered-fields can be captured which is not possible with classical FTL. In theory, as far as the wires of the MTL can entirely be included in a fictitious surrounding cylinder, each current on each wire should independently contribute to the update of the scattered EM-field on the surface of the cylinder. From this perspective, the compactness of the electric wires in cable-bundles is an advantage because the scattered EM-field update can advantageously be made by the total current on the bundle, which is a reasonable approximation from physics point of view and an efficient approximation from numerical implementation point of view. This approximation is all the more relevant if we consider the fact that the exact position of wires generally changes all along the bundle routes, naturally producing an averaging of the total current on the bundle. In order to calculate the required equivalent total field, we thus suggest to replace the bundle by an equivalent wire and to model it as a thin-wire in a 3D-full wave model as made on the previous single-wire test-cases.

To this extent, we can propose an appropriate modelling strategy for extending our modified-FTL model to MTLNs. For each cable-bundle, we consider the following steps:

- We define an equivalent wire model of the cable-bundle,
- We calculate the equivalent total EM-field with a thin-wire model of the equivalent wire model of the cable-bundle according to (29),
- We calculate the k_L factor as in (32) based on the equivalent wire model of the bundle,
- We calculate the p.u.l. parameters referenced to the closest 3D surface approximated to an infinite ground-plane as usually done for FTL,
- We apply the multiplication by the k_L factor on the p.u.l. resistance matrix terms and the equivalent total field to obtain the modified-FTL source-term as in (34)
- We apply this total field as source term on the MTLN model of the cable-bundle harness as we would do it in a regular FTL-modelling process.

In addition, we complete the MTLN model, applying the multiplication by the k_L factor on all end-impedances at end-junctions as mentioned in paragraph II.F.

Thereby, our problem of extension of the modified-FTL model to MTLs is now transferred to the problem of being able to define a simplified equivalent wire model of cable bundles. Several references have already investigated this problem, from equivalent wire models or simplified MTL models points of view ([22], [23], [24]). They all conclude that perfectly equivalent models do not exist except in specific conditions of MTL-end-loads and excitations. However, efficient approximations exist for cable-bundle configurations and may give very acceptable results for common-mode excitations such as for EM-field illumination. Especially, it may be showed that, at high frequencies, the total cable-bundle current (also called sometimes "common-mode" total current) behaves as a single-wire-TL for which p.u.l. and end-load parameters can be calculated with simple summation rules of the terms of the p.u.l. electrical matrices [24].

Finally, we expect to be able to keep using FTL in the low frequency range (below the one or two first resonances of the cable-bundle) because its validity has been proved for a long time and to use the modified-FTL model in the high

frequency range (over the one or two first resonances). The objective of the next paragraph is to validate this conjecture.

B. MTL VALIDATION SCOPE

Nevertheless, the validation of the above mentioned conjecture raises the question of the availability of reference results. As far as cable-bundles are concerned, the only real reference should be provided by measurements. Only measurements allow access to currents on elementary cable-wires but they raise other issues. One of them is confidence in the measurement results themselves because of their complexity, the difficulty to control the positions of wires inside cable-bundles. Besides, the difficulty is to define geometrical and electrical configurations general enough to avoid drawing test-case-dependent conclusions. Especially we do not want to forget our final objective that is to be able to address real industrial complexity problems for which well-documented measurements are very rare.

For all those reasons, we decided to focus on EM-simulated reference results and we decided to take the opportunity of an available simulation model of a real aircraft to carry out our validation. Of course, to our knowledge, except FTL with the limitations reminded in this article, there is no numerical solution capable to address the complexity of industrial wiring test-cases. This is why we have adopted the following comparison strategy to assess the relevance of our results:

- The comparison between the three methods will be done on total currents, equal to:
  - ° The sum of all currents on elementary wires in both the FTL and modified-FTL methods,
  - ° the current calculated with the full-wave method on the thin-wire model of the bundle equivalent wire,
- At low frequency, the reference results will be provided by the FTL results,
- At high frequency, the reference results will be provided by the equivalent single-wire-TL model.

This validation strategy allows us to consider the comparison of total currents obtained with the three modelling methods previously used for the generic single-wire test-cases (full-wave, FTL and modified-FTL methods).

C. APPLICATION TO AN INDUSTRIAL COMPLEXITY TEST-CASE

The chosen MTLN validation configuration thereby concerns the simulation model of a real aircraft: Dassault-Aviation's RAFALE fighter aircraft. The validation concerns a numerical simulation work performed in the frame of a French Defence national project called "MOVEA2" for which one of the subject was to assess HIRF (High Intensity Radiated Fields) [25] EM-coupling onto the aircraft wiring. All the details concerning the building of the aircraft-model cannot be disclosed in this paper, some for confidentiality reasons and others because of the huge size of the problem. However, the results presented in this paragraph should give the reader a good idea of today's capability, ready to be achieved with both FTL and modified-FTL methods, on such large industrial problems. In this work, the HIRF analysis has been carried out on a specific harness of the whole aircraft wiring. It will be called in this article "TEST-BUNDLE". This wiring extends in the whole aircraft, in the fuselage and in the wings. Fig. 10 presents its topology in which the size of the drawn-lines depends on the real cross-section dimensions of the cable bundles. The bundles contain a large variety of cable types (single wires, wire-pairs, three-wires cables, shielded and unshielded cables). The biggest bundle has 127 pin contacts at the level of its equipment connector.

The HIRF excitation is simulated with a plane wave made of a Gaussian time-domain waveform with a frequency spectrum large enough in order to comply with the quasi-TEM validity of the MTL models of the problem. In particular, the 300 MHz upper frequency is in accordance with the maximum average height of the bundles with respect to the reference structure. All currents results have been normalized to the Gaussian waveform.

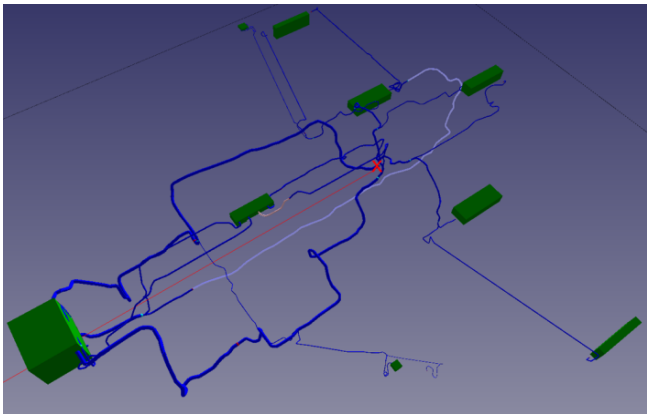

FIGURE 10. View of the TEST-BUNDLE wiring inside Dassault-Aviation's RAFALE fighter aircraft (courtesy Dassault Aviation).

The approach followed in the analysis is the following:

- Generation of the aircraft FDTD mesh (NASH software [26]). The aircraft is about 15m long for the fuselage and 10m wide for the wing span. This 3D model includes all types of structural losses (materials, contact impedances, seams…). The cell size is 2 cm.
- Thin-wire models and results:
  - o Meshing of the whole wiring as oblique thin-wire models with a fixed 12 mm maximum diameter imposed by stability criterion constraints and inclusion in the FDTD model of the aircraft structure (CableSim software [27]).
  - o 3D FDTD calculation on all the wires of the TEST-BUNDLE (TEMSI-FD software [19]). This calculation has been made on the high power computing resources available at Dassault Aviation,
- FTL models (classical and modified):

  - Meshing of all the wiring except the TEST-BUNDLE part as oblique thin-wire models and inclusion in the aircraft FDTD model
  - MTLN modelling of the TEST-BUNDLE network (CableSim software)
  - FDTD calculation of the source fields required by the FTL models along the central paths of the TEST-BUNDLE wiring (TEMSI FD software)
- FTL and modified-FTL calculations of the TEST-BUNDLE (CRIPTE software [20])

In the FDTD model, the thin-wire network has the same topology as the real cable network. Note that this model is all the more relevant due to the large number of low-impedance cable-bundles that include shielded-cables and cable overshields in military aircraft. The k_L factor (32) is calculated from this thin-wire network model. The inductance of the Inner-TL, $L_{TL,int}$, is calculated from the oblique thin wire model embedded in the TEMSI FDTD solver. The equivalent total field distribution is directly equal to the total field quantity generated by this oblique thin wire model in the FDTD solver. The cylinder used for averaging the scattered field is made by the various cubic cells crossed by the oblique thin-wires.

In terms of computer resources, the FDTD meshed model is made of about 250.10^6 2cm-cubic cells, leading to 25Gb of memory ($1.5.10^9$ unknowns). The computation has been made on a Dassault's supercomputer with a total CPU-time of about 28 h for $5.2.10^6$ time steps of about 20 ps up to a maximum time of 0.1ms. This CPU-time does not vary significantly between the two FTL-oriented computation and the Full FDTD computation. However, the advantage of the FTL oriented computation is that it may support any type of MTLN model ranging from simplified thin wire to real multiconductor cable-networks as well as different models of sources terms in our specific case. Whereas the 3D computation requires tens of hours on a super computer, the MTLN calculations only requires 1 hour for the TEST-BUNDLE MTL model on a standard workstation for some hundreds of calculated frequencies. Such a computation time difference shows the interest of the FTL methods (classical or modified) as far a sensitivity analysis on the topology of the wiring is concerned.

In Fig. 11, we present the comparisons of the cable-bundle total currents simulated at the level of three connectors named "162F", "108C" and "109C" with the two FTL methods (classical and modified) and the full-wave reference method. Note that impedance conditions at connector "162F" are high-impedance whereas they are low-impedance at the two other connectors. This will have an impact on the comparisons between the three modelling methods for which comparison assessment will have to be made having in mind the following limitations:

- The very low frequency responses are not available since results are presented from 1 MHz only. Indeed, all time-domain signals could not correctly be damped to zero at long enough times due to the demanding high-resources of 3D calculations,
- The reference thin-wire model is not a perfect reference. The MTLN model instead involves elementary wire dimensions, real materials of wires, real connections at junctions. The end-loads of the thin-wire model have been all approximated to short-circuits whereas the MTLN model accounts for real circuit-networks at equipment connectors. Consequently, the thin-wire model cannot catch the real MTLN topology especially because it imposes Kirchhoff's nodes at wire-junctions. In addition, the thin-wire models may have a diameter smaller than the real bundle diameters (so the thin-wire p.u.l. TL parameters do not always match the TL parameters that would have been calculated by summation rules of the p.u.l. MTL parameters [24]).
- The equivalent total field of the modified-FTL model had to be calculated with this thin-wire model approximation of the bundle, despite its approximation.
- A frequency sweep window averaging of 5% has been applied on all current results as recommended for measurements in the ED107 standard [25] (when step-by-step frequency sampling is used, such an averaging technique lowers the risk to miss resonance frequencies and mitigates possible errors on resonance peak amplitudes).

All those limitations and process-practises have an impact on the low frequency (under the resonance regime) parts of the comparison plots in Fig. 11. Even if the comparisons start at 1 MHz, we see that the agreement between FTL and modified-FTL is quite good up to the first resonance despite some Fourier transform issues still observable at those frequencies in the modified-FTL model. However we also observe that the full-wave method results are always higher, which confirms the non-relevance of the thin-wire model at low frequency.

At high frequencies (in the resonance regime), the nature of discrepancies observed at low frequency between the Full-wave method and the two FTL methods is not relevant anymore, due to the property that the total currents behave similarly as for homogeneous equivalent wires. Nevertheless, as far as FTL is concerned, we observe that this agreement is not always perfect.

At connector 162F for example, the high frequency agreement of FTL with the two other methods is particularly good because EM-radiation losses are insignificant compared to resistive end-load due to the high-impedance condition mentioned above, for the same reason as the 50 Ω configuration in Fig.9's single-wire test-case. However, for connectors 108C and 109C, we observe that the peak amplitudes obtained by FTL are much higher because EM-

radiation losses are significant compared to end-load losses whereas, in the full-wave and the modified FTL methods, the agreement is very good. Besides, we see that the impact of using a thin-wire diameter, not always in accordance with the real bundle diameter, does not seem to have a significant error impact on the precision of the equivalent total EM-field source terms.

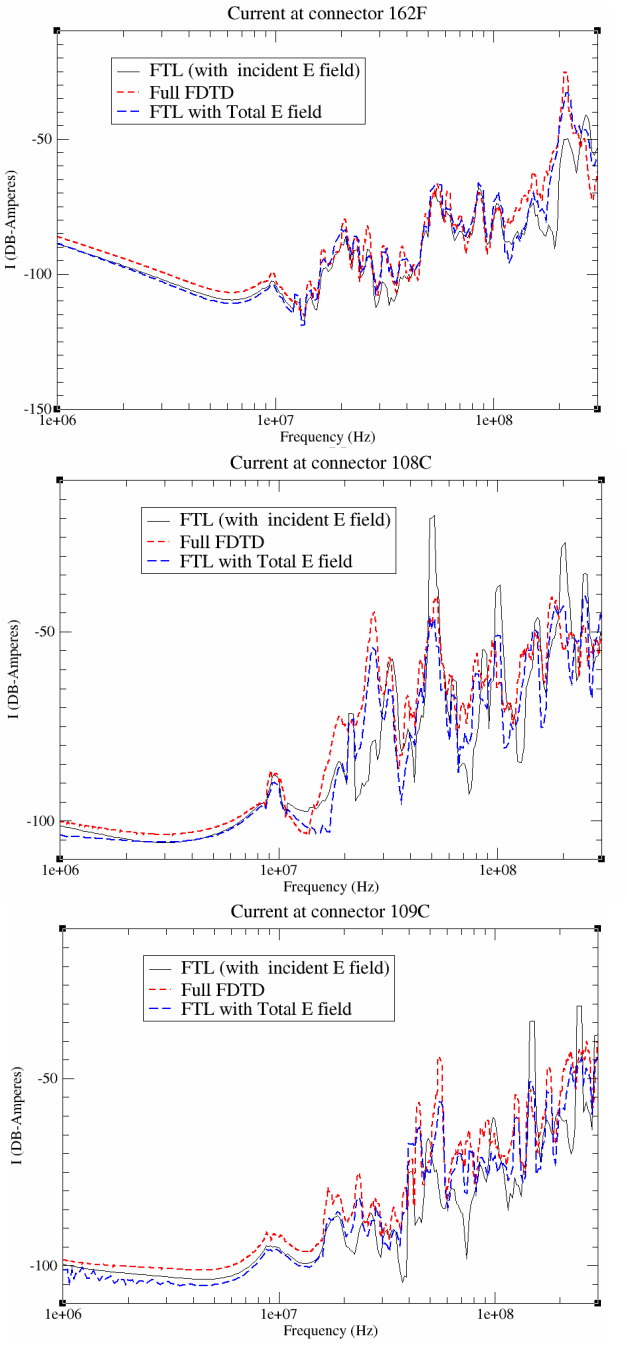

FIGURE 11. View of the TEST-BUNDLE wiring inside Dassault's RAFALE fighter aircraft. Comparisons of currents obtained between full-3D label "Full FDTD"), classical Agrawal's method (label "FTL (with incident E field)") and modified-FTL method (label "FTL with Total E field").

V. FUTURE PROSPECTS

This work is the first publication on the modified-FTL model and several evolutions of this research work can be proposed in order to confirm its relevance for EM-coupling on cable-bundle problems. First, future work on this subject should address the precise equivalent wire models to be derived for the equivalence of bundle total currents. Especially, even if the simple thin-wire model used in the aircraft fighter application shown in this article has given very encouraging results, despite crude approximations, the sensitivity of the equivalent thin-wire model to bundle radii and values of end-impedances will need deeper investigation.

Another possible evolution of the application of the modified-FTL model could consist in choosing the geometry of the cylinder in order to evaluate in a simple way the p.u.l. parameters of the inner-TL. A circular cylinder shape would be the simplest choice allowing easy determination of the equivalent coaxial inner-TL p.u.l. electrical parameters and, therefore, of the k_L factor. Doing so, the difficulty of the problem would be transferred to the problem of being able to precisely calculate the EM-fields on the circular-cylinder surface. Future work should investigate the interest of such an approach.

Besides, the requirement of the definition of a fictitious cylinder for the determination of the equivalent total field could be also possibly avoided applying the technique known as "test-wire" technique [28]. This technique provides an evaluation of the source terms to be applied on a TL model thanks to the knowledge of the distribution of currents along test-wires. The test-wires are very similar to the equivalent wires used in the modified-FTL model. From a practical 3D-calculation point of view, the collection of the distributed currents along the equivalent wire could be easily made. Future work should thereby evaluate to which extent, such a test-wire technique might allow getting rid of this fictitious cylinder concept.

VI. CONCLUSION

In this paper, we presented a modified-FTL model in a frequency-domain formulation and made an analogy to Agrawal's well-known FTL model. The main advantage of this modified model is that it includes the reaction of the wire induced-currents on the scattered EM-fields. The formulation has been obtained by the derivation of the first TL-equation of the well-known Agrawal-FTL demonstration on a single-wire-TL made of a signal-wire and a return-wire. The second TL-equation is not modified. This derivation leads to the definition of a specific TL-model with specific excitation terms. Whereas the TL-model in the classical FTL is made of the signal-wire with respect to the return-wire, the derived modified-TL-model is made by the signal-wire with respect to a fictitious surrounding cylinder acting as a return-conductor. The excitation source term is defined as an equivalent "total" electric tangential field equal to the usual incident tangential electric field plus an average of the scattered tangential electric fields on the surface of the surrounding cylinder. As a matter of facts, this derived FTL

model appears as a frequency-domain formulation of the well-known time-domain Holland model (or its derivatives for oblique wires). Nevertheless, the specificity of this frequency-domain model is to allow the process of exchange and update of EM-fields to be made a-posteriori instead of at each calculation time.

The analogy of the derived-FTL model with Agrawal's model requires considering p.u.l. TL-parameters referenced to the real return-conductor since the end-loads of the TL are connected to this return-conductor. This is mathematically obtained by multiplying all terms of the two equations of the derived FTL model by a k_L factor equal to the ratio of the p.u.l. inductances of the classical and derived-TL models. The equations of the modified-FTL are then obtained. As for Agrawal's model, the TL model is thereby referenced to the 3D structure. Moreover it can run independently from the 3D model and it can be applied with usual FTL procedures and tools. The differences with Agrawal's FTL model are:

- The excitation term depends on the wire and is equal to the equivalent "total" tangential electric field multiplied by the k_L factor,
- The p.u.l. resistance of the TL with respect to the 3D structure as well as the TL end-impedances are also multiplied by the k_L factor,
- An equivalent voltage is defined along the TL. As for Agrawal's scattered voltage, this voltage is not used as such since its definition is quite complicated and not related to a real voltage. Only the current is practically used in this model.

Validations of the modified FTL-model have been made on fully controlled generic test-cases made of single-wire networks running over PEC ground planes for both EM-field and direct wire excitation configurations by computing EM-source fields with a FDTD model. The results have been compared with full-3D calculations in which the single-wires were parts of the 3D mesh as thin-wire models.

The extension of the modified-FTL model to MTLs relies on the existence of an equivalent single-wire model of each bundle. The thin-wire model of this equivalent wire is then used in a 3D model for the numerical evaluation of the total equivalent tangential electric field distribution and analytical evaluation of the k_L factor. Consequently, in the calculation process derived from the modified-FTL model and unlike in FTL model, the equivalent thin-wire models have to be present in the 3D full-wave model for the equivalent total field calculation. However, like in FTL, any type of cable network topology can then be modelled with the same equivalent field terms, provided that the equivalent wires have the same routes as the routes on which the equivalent total fields have been determined and provided that the equivalent thin-wire model used for the determination of those fields is supposed unchanged.

In order to demonstrate the operative aspect of this process, an application of this MTL extension has been made on an industrial complexity test-case (a wiring part of Dassault-Aviation's RAFALE fighter aircraft) offering the evaluation of the capabilities of the method on a real MTLN configuration in a real 3D environment. Because of the absence of reference numerical models of bundles, the comparisons were limited to total bundle currents in FTL and modified-FTL on the one hand and thin-wire model on the other hand. The results point out the interest of this method at high frequencies, especially for resonance peak evaluation since the modified-FTL approach implicitly accounts for EM radiation losses. Consequently, we can propose the following share of FTL models in a wide frequency band process for modelling EM-coupling on a wired complex-system:

- Use Agrawal FTL method in the low frequency (under the cable bundle resonances)
- Use the modified-FTL model at high frequencies (in the resonance region of the cable-bundle response).

ACKNOWLEDGMENT

The authors want to thank Mr. Christophe Migeon from the French Defence Delegation to Armament to have given his approval for the publication of the MOVEA2 results on the RAFALE fighter aircraft.

REFERENCES

[1] F.M. Tesche, M.V. Ianoz, T. Karlsson, "EMC Analysis Methods and Computational Models", *John Wiley & Sons*, pp.247–266. 1997.

[2] C. R. Paul: "Analysis of Multiconductor Transmission Lines", *John Wiley and Sons*, 1994.

[3] C. E. Baum, T. K. Liù, F. M. Tesche, "On the Analysis of General Multiconductor Transmission-Line Networks", *Interaction Notes*, Note 350, November 1978, [Online]. available : http://ece-research.unm.edu/summa/notes/.

[4] A.K. Agrawal, H.J. Price and S.H. Gurbaxani, "Transient response of multiconductor transmission-line excited by a nonuniform electromagnetic field", *IEEE Trans. Electromagn. Compat.*, vol. 22, no. 2, pp. 119–129, May 1980.

[5] C.D. Taylor, R.S. Satterwhite and C.H. Harrison, "The response of a terminated two-wire transmission line excited by a nonuniform electromagnetic field", *IEEE Trans. Antennas and Propag*., vol. 13,no. 6, pp. 987–989, 1965

[6] F Rachidi, "Formulation of the field-to-transmission line coupling equations in terms of magnetic excitation field", *IEEE Trans. Electromagn. Compat.*, vol. 35, no. 3, pp. 404–407, Aug. 1993.

[7] L. Paletta, J-P. Parmantier, F. Issac, P. Dumas, J.-C. Alliot, **"**Susceptibility analysis of wiring in a complex system combining a 3-D solver and a transmission-line network simulation", *IEEE Trans. Electromagn. Compat.*, vol. 44, no. 2, pp. 309–317, May 2002.

[8] X. Ferrières, J-P. Parmantier, S. Bertuol, A. Ruddle, "Application of hybrid finite difference / finite volume to solve an automotive problem", *IEEE Trans. Electromagn. Compat.*, vol 46, no 4, pp. 624–634, Nov. 2004

[9] E. Bachelier, S. Bertuol, J-P. Parmantier, T. Volpert, D. Roissé, N. Muot, C. Giraudon, C. Girard, "HIRF-SE Cooperative EM Simulation Approach for Modeling the NTC1 Test-case with the ALICE FDTD and CRIPTE Codes", *proceedings of CEMEMC'13 workshop*. March 19th-21st, 2013

[10] S. Arianos, M. A. Francavilla, M. Righero, F. Vipiana, P. Savi, S. Bertuol, M. Ridel, J-P Parmantier, L. Pisu, M. Bozzetti and G. Vecchi, "Evaluation of the modeling of an EM illumination on an aircraft cable harness", *IEEE Trans. Electromagn. Compat*.,vol. 56, no. 4, pp. 844–853, Aug 2014.

[11] FAA Advisory Circular "Certification of Electrical Wiring Interconnection Systems on Transport Category Airplanes", AC no. 25.1701-1
[12] R. Holland and L. Simpson, "Finite-difference analysis of EMP coupling to thin struts and wires," *IEEE Trans. Electromagn. Compat.*, vol. 23, no. 2, pp. 88–97, May 1981.
[13] C. Guiffaut, A. Reineix and B. Pecqueux, "New oblique thin wire formalism in the FDTD method with multiwire junction," *IEEE Trans. Antennas and Propag.*, vol. 60, no. 8, pp. 1458–1466, Mar. 2012.
[14] C. Guiffaut, N. Rouvrais, A. Reineix and B. Pecqueux, "Insulated oblique thin wire formalism in the FDTD method," *IEEE Trans. Electromagn. Compat.*, vol. 59, no. 5, pp. 1532–1540, Oct. 2017.
[15] F. Edelvik, "A new technique for accurate and stable modeling of arbitrarily oriented thin wires in the FDTD method," *IEEE Trans. Electromagn. Compat.*, vol. 45, no. 2, pp. 416–423, May 2003.
[16] J.-P. Berenger, "A multiwire formalism for the FDTD method," *IEEE Trans. Electromagn. Compat.*, vol. 42, no. 3, pp. 257–264, Aug. 2000.
[17] J-P. Parmantier, X. Ferrières, P. Schickele, A Hybrid Time-Domain Maxwell/MTLN-Equations Method to Simulate EM-induced-Currents on Electric Cable-Bundles Inside Cavities, Advanced Electromagnetics, Vol.9, N°. 2, August 2020
[18] P. Degauque et J-P. Parmantier, "Chapitre 2 : Couplage aux structures filaires" in "Compatibilté Electromagnétique", *Collection technique et scientifique des télécommunications, Lavoisier*, Hermes. Paris 2007.. In French.
[19] "Time ElectroMagnetic Simulator – Finite Difference software", TEMSI-FD, *CNRS*, *Univ. of Limoges*, Limoges, France, 2017 version.
[20] J. P. Parmantier, S. Bertuol, and I. Junqua,"CRIPTE : Code de réseaux de lignes de transmission multiconducteur", User's guide – Version 5.1" ONERA/DEMR/T-N119/10 - CRIPTE 5.1 2010.
[21] E. F. Vance, "Shielding cables", *Wiley* 1978, ISBN 10: 0471041076
[22] C. Poudroux, M. Rifi, and B. Démoulin, "A simplified approach to determine the amplitude of transient voltage on the cable bundle connected on non linear loads", *IEEE Trans. Electromagn. Compat.*, vol. 37, no. 4, pp. 497–504, Nov. 1995.
[23] G. Andrieu, L. Koné, F. Bocquet, B. Démoulin, J-P. Parmantier, "Multiconductor reduction technique for modeling common mode current on cable bundles at high frequency for automotive applications", *IEEE Trans. Electromagn. Compat.*, vol 50, no 1, Feb. 2008.
[24] J-P. Parmantier, I. Junqua, S. Bertuol, F. Issac, S. Guillet, S. Houhou, R. Perraud, "Simplification method for the assessment of the EM response of a complex cable harness", in *Proc. 20th Int. Zurich Symp.- Electromag. Compat.*, Jan. 12–16, 2009.
[25] *"*Guide to Certification of aircraft in a high-intensity radiated field (HIRF) environment*"*, *EUROCAE ED 107 Revision A*, July 2010.
[26] "NASH software", Axessim, [Online]. Available at https://www.axessim.fr/nash-1606-released.html.
[27] "CABLESIM software", *Axessim*, [Online]. Available at https://www.axessim.fr/cablesim.
[28] J.P. Parmantier, "The test-wiring method", *Interaction Notes*. Note 553. October 1998 (available at http://ece-research.unm.edu/summa/notes/).